Papp, I.; Sieben, C.; Sisson, A.L.; Kostka, J.; Boettcher, C.; Ludwig, K.; Herrmann, A.; Haag, R.:

Inhibition of Influenza Virus Activity by Multivalent Glycoarchitectures with Matched Sizes

In: ChemBioChem (2011) Wiley

DOI: 10.1002/cbic.201000776

DOI: 10.1002/cbic.201000776

Inhibition of Influenza Virus Activity by Multivalent Glycoarchitectures with Matched Sizes

Ilona Papp,[§[a]] Christian Sieben,[§[b]] Adam L. Sisson,[[c]] Johanna Kostka,[[b]] Christoph Böttcher,[[d]] Kai Ludwig,[[d]] Andreas Herrmann,[[b]] and Rainer Haag[[a]*]

We describe the synthesis of a series of sialic acid conjugated, polyglycerol based nanoparticles with sizes in the range of 1–100 nm in diameter. Particle sizes were varied along with the degree of functionalization to match the corresponding virus size and receptor multiplicity in order to achieve maximum efficiency. To build up these architectures, we used as scaffold the biocompatible hyperbranched polyglycerols and recently developed polyglycerol based nanogels of which sizes can be varied between 2–4 nm and 40–100 nm, respectively. We demonstrate that such multivalent nanoparticles are inhibitors of virus-cell binding, virus-cell fusion, and consequently, infectivity. The potential of multivalency is evident from larger particles showing very efficient virus inhibition up to 80%. Indeed, both the size of the nanoparticle and the ligand density are important determinants of inhibition efficiency. The inhibitory activity of the tested polymeric nanoparticles drastically increased with the nanoparticle size. Particles of dimensions similar to that of virus (50–100 nm) are exceedingly effective. We also observed a saturation point in degree of surface functionalization, i.e. ligand density, above which inhibition was not significantly improved. Our study emphasizes the importance of matching particle sizes and ligand densities to mimic biological surfaces and improve interactions; this is a vital concept underlying multivalent interactions.

Introduction

Influenza virus causes epidemics and pandemics in human populations, and eradication of the disease will be difficult to achieve. The two envelope glycoproteins hemagglutinin (HA) and neuraminidase (NA) determine the viral subtype and mark the major targets for human immune response. HA mediates cell attachment by binding sialic acid (SA) residues on glycoproteins and glycolipids. NA catalyzes the cleavage of terminal SA and allows progeny viruses to leave the cell.[1] The virus genome is composed of 8 segments and underlies a high mutation rate. This causes alterations in HA and NA which leads to altered antigenicity and is responsible for episodic recurrence of influenza.

Current vaccines against influenza do not provide a satisfying solution since they require several months of preparation and their effects are often controversial.[2] Alternatively, during the past two decades many drugs were investigated that are designed to suppress viral replication post infection. Most commonly, these drugs target either the neuraminidase activity (Zanamivir/Relenza® and Oseltamivir/Tamiflu®),[3] which have reached the market, or the proton channel M2 (Amantadine/Symmetrel® and Rimantadine/Flumadine®).[4] However, the emergence of stable and transmissible drug resistant influenza strains can render these drugs ineffective.

An alternative to inhibit influenza replication is to target HA[5] and thereby prevent viral adhesion; however, those compounds failed to become drugs. This was mainly due to weak HA binding properties shown by monomeric sialic acid derivatives.[6] The viral adhesion uses a multivalent effect since monovalent binding between HA and SA is weak with dissociation constants in the millimolar range.[7] Hence, a high fraction of the ~300 HA spikes per virus must interact cooperatively to attach the virus to the host cell membrane. The application of free SA as a competitive inhibitor of viral adhesion is not a viable option as the effective concentration required is too high to be tolerated systemically.[8] Therefore, a pioneering strategy to append multiple representations of sialic acid residues on therapeutic polymers to achieve high local concentrations was introduced more than 15 years ago.[4b, 5, 7]

The synthesized synthetic HA inhibitors reported to date have been low molecular weight scaffolds forming clusters of monovalent,[6, 8-9] bivalent,[10] tetravalent,[11] and octavalent (used scaffold was a polyazido-calix[4]arene)[12] sialosides.

Two types of carriers were adopted for obtaining glycoconjugates bearing multiple sialic acid residues: natural backbones such as self-assembling sialo-glycopeptides,[13] proteins[14] or polysaccharides[15] and synthetic backbones in

[a] *I. Papp, Prof. R. Haag*
Freie Universität Berlin, Institut für Chemie und Biochemie
Takustraße 3, 14195 Berlin (Germany)
Tel: +493083852633; Fax: +493083853357
Email: haag@chemie.fu-berlin.de

[b] *C. Sieben, J. Kostka, Prof. A. Herrmann*
Humboldt-Universität zu Berlin, Institut für Biologie/Molekulare Biophysik; Invalidenstraße 42, 10115 Berlin (Germany)

[c] *Dr. A. L. Sisson*
GKSS Forschungszentrum Geesthacht
Kantstraße 55, 14513 Teltow-Seehof (Germany)

[d] *Dr. C. Böttcher, Dr. K. Ludwig*
Freie Universität Berlin, Institut für Chemie und Biochemie
Forschungszentrum für Elektronenmikroskopie
Fabeckstraße 36a, 14195 Berlin (Germany)

[§] *Both authors contributed equally to this work.*

Supporting information for this article is available on the WWW under http://www.chembiochem.org or from the author.

terms of spherical (dendrimers[16] and liposomes[17]), linear polymers, and nanostructures.[13, 18] The vast majority of amorphous linear polymers used were either copolymers of acrylamide esters used by Roy,[19] Whitesides,[20] Bovin,[21] Matrosovich,[5, 22] Watson,[23]; or copolymers of acrylic acid esters;[20c, 24] polystyrene,[25] and others.[26] Here multivalency offers some major advantages. The entropic penalty of the ligand to escape the bound state is decreased which means that the macroscopic dissociation rate is much lower than in the monomeric situation. After a single point dissociation occurs there is a high rate of re-association for each ligand. However, serious concerns have been raised about the toxicity of polymeric sialosides having polyacrylamide backbones.[4b]

In this paper, we describe a facile strategy to design stable and biocompatible glycoconjugated nanoparticles. By using glycoarchitectures with defined size (3, 4, 50, and 70 nm) we achieved strong inhibition of influenza virus activity, depending on particle size and degree of SA functionalization. The use of water soluble polyglycerol nanoparticles as scaffolds for SA has many advantages: they can be synthesized easily with good control over polydispersity[27] and in good yields; are more flexible than dendrimers, have excellent solubility, compared to linear polymers, and certain a higher level of terminal end group functionality.[28] We applied biophysical and biological methods to investigate the effect of functionalized polymeric nanoparticles on influenza virus binding, fusion activity and infectivity.

Results and Discussion

Herein we describe a new approach by coupling multiple SA residues to water soluble, biocompatible polyglycerol nanoparticles on different length scales. Influenza viruses are enveloped and are pleiomorphic (i.e. they can vary their size and shape). Since viruses isolated from cell culture are typically spherical, with a constant diameter of ~100 nm[29] we varied the polymeric particle sizes along with the degree of functionalization to match the corresponding virus size. The strength of our approach is that the multivalent substrate used is a neutral, hydrophilic, branched polyether which can be considered comparable to the widely used PEG based materials with regards to toxicity and biocompatibility.[30]

This new class of multivalent glycoarchitectures inhibits influenza virus function by perturbing the HA working cycle, as proved by various biophysical approaches to investigate virus activity. We present evidence that multivalent inhibitors reduce the viral activity by up to 80%.

Synthesis of the sialylated nanoparticles. Hyperbranched polyglycerols (hPGs) are a class of water soluble, dendritic,[31] biocompatible polyether-polyols.[30b] hPGs are typically prepared by ring opening multibranching polymerization of glycidol either by cationic[32] or anionic[27a, 33] means. There are many examples of polyglycerol materials being used in numerous biomedical applications, with potential uses anticipated to be found in a wide range of situations as other hydrophilic polyethers such as polyethyleneglycol.[28b] One advantage of hPG is its dendritic structure. This results in a globular polymer with a high density of hydroxyl end groups which can be further functionalized by established chemical methods. We recently showed that galactose functionalized hPG were ideal scaffolds for multivalent presentation of galactose units for in vitro selectin binding.[34] By that, we became aware of the potential to prepare sialic acid decorated analogs and evaluate their ability to bind viral surfaces. hPG decorated with sulfate groups were compared in our study, as it was hypothesized that a polyanionic surface may also mimic a multivalent SA array.[35] Notably, hPGs used in our study were of the order of 3 kDa molecular weight with respective diameters of 3–4 nm.

Particles of this size may present a maximum of up to 40 sialic acid moieties in a multivalent array on the surface. In order to prepare polyvalent architectures of increased dimensions, polyglycerol nanogels (nPGs) were prepared with surfaces decorated by sialic acid. nPGs are recently reported polyglycerol materials which are a magnitude larger in diameter than hPGs, with sizes varying between 25 nm and 100 nm in diameter. As a new class of hydrogel, nPGs are not strictly dendritic, but they are comparable to hPGs with a globular structure and polyhydroxylated surface which is readily functionalizable.[36] The nPG nanoparticles are comparable in size to individual influenza particles and can consequently interact with the virus over a vastly increased surface area. Also, a new concept of matched size and functionality to achieve an optimal biosurface interaction is introduced.

Figure 1 shows the general structure of the 6 synthesized substrates used in this study. Structures **1**–**4** are based upon a hPG core of average molecular weight 3 kDa.[27] Sialic acid residues in structures **1**–**3** were attached to the surface via triazole linkage by standard Sharpless/Huisgen click chemistry.[37] Initially, a fraction of free hydroxyl groups on the hPG core were converted to propargyl ethers with controlled and varied degrees of functionalization (see Table 1). An azide functionalized sialic acid derivative[20b, 38] was subsequently conjugated to each hPG core in an overall highly efficient process based upon protocols previously developed within our group.[34] Structure **4** does not contain any sugar units on the surface, and was prepared by simple sulfation of the hydroxyl groups of a 3 kDa hPG core in high conversion as previously reported.[35]

The larger nPG nanoparticles **5**–**6** were prepared by conjugating azide containing polyglycerol nanoparticle cores with propargyl functionalized sialic acid residues, again by employing standard click chemistry. Azide bearing polyglycerol nanogels were previously developed by us in a process using the inverse miniemulsion templated acid catalysed ring opening polymerization of glycerol triglycidyl ether.[36c] The miniemulsion conditions could be controlled to modify the size of prepared particles from 20 nm to 100 nm with relatively narrow size dispersion. Azides with varying degrees of functionalization could be incorporated onto the preformed nanogels in an additional nucleophilic ring opening of unreacted glycidyl epoxides with sodium azide. Direct evidence for the size and spherical morphology of polyglycerol particles as well as their azide activated analogs was obtained by cryo–transmission electron microscopy. Corresponding micrographs (Figure 2) and more comprehensive preparative details are provided in the experimental section.

As shown in Table 1, sialic acid containing hPGs **1**–**3** were prepared with functionalization degrees of 15, 50, and 90%, respectively. This equates to 6, 20, and 35 sugar units per individual macromolecule. NMR analysis was used to quantify the degree of functionalization (DF) in each case. Molecular weights of the final sugar conjugated polymers were calculated on the basis of DF (Table 1). Each of these polymers had a measured diameter of 3–4 nm by dynamic light scattering (DLS). Similar analyses on sulfated hPG analogue **4** revealed a degree of functionalization of 85% or approximately 32 sulfate groups per macromolecule; the sulfur content was determined by elemental analysis. The particle sizes of nanogels **5** and **6** were determined as 50 nm and 70 nm in diameter, by DLS, respectively.

From our previous experience with polyglycerol nanogels prepared in miniemulsion we estimated the molecular weights of such polymers to be in the order of 10^4 kDa. NMR analysis was used to quantify the proportion of sugar units relative to backbone structural repeat units (glycidols). Therefore, it was possible to calculate the number of sugar units relative to estimated molecular weights as shown in Table 1. It is important to note that for the purposes of the following influenza binding and fusion studies, comparisons between polymers were made on a per sialic acid basis, not on a per particle basis. Therefore any increases in binding when observed from a per sialic acid reference must presumably arise from multivalency effects. This also means that absolute molecular weights are not required for nPGs **5** and **6** as our measured sialic acid:glycidol ratios are constant and independent of absolute molecular weight.

Biological Assays.

We applied biological and biophysical methods to evaluate the effect of the above mentioned sialylated polymeric nanoparticles on influenza virus activity.

Binding Inhibition. Initially, we investigated the ability of such polyglycerol constructs to act as inhibitors of HA binding to erythrocyte target membranes. For this we labeled influenza A (strain A/X31) virus with the fluorescent lipid analog R18. Labeled virus and washed human erythrocytes were incubated for 30 min and unbound virus was removed by centrifugation. The amount of bound virus per erythrocyte was measured by flow cytometry as the mean R18 intensity. To study inhibitory strength, viruses were preincubated with our substrates **1**–**6** in varied concentrations. Figure 3 summarizes the results on binding experiments. To express the effect of multivalency, monovalent sialic acid was used as an inhibitor reference in all experiments. The monomeric form of sialic acid had no effect on the viral adhesion between 400 μM and 4 mM. In contrast preincubation of influenza virus with sialic acid functionalized hPGs **1**–**3** led to a strong reduction of fluorescence signal per erythrocyte. Binding was inhibited to 50% of control level at approximately 3 mM (SA equivalent) concentrations of hPGs but significant reductions in virus binding were observed as low as at 1 mM. A significant difference was not observed in inhibitory effect between the series **1**–**3** with varied degrees of functionalization. This implies a rather linear dependence on the multivalent effect of SA binding to HA at least in the range of this experiment. To make a very simplified evaluation, polymer **3** (35 sugar units) bound approximately 6 times stronger than polymer **1** (6 sugar units). Therefore, in this series, each subsequent SA moiety contributed equally (on average) to overall inhibitory strength. Much greater inhibitory effects per sialic acid were observed with the larger nPG **5**, as can be seen in Figure 3.

On a per sialic acid basis, construct **5** exhibited 50% inhibition at concentrations of some 40-fold lower than the hPG series at approximately 4 mM SA equivalent concentration. This equates to a markedly exponential increase in binding strength with greater particle size and number of multivalent binding units. In comparison, nPG **6**, which differs by degree of functionalization, showed weaker inhibition. Nanoparticle **6** has a DF of 80% whereas nanoparticle **5** has a reduced DF of 12%. As a general trend, which was also observed in our earlier work with selectin binding,[14] we found that a greater surface density of ligand groups led to losses in binding efficiency, when compared on a per ligand basis. It would be rational to assume an optimum spacing distance between ligands for maximum efficiency in binding per ligand. This effect seems to be even more the case among the nPG series **5**–**6** relative to the hPG series **1**–**3**. It can be hypothesized that particles bearing several thousand SA units form very tight complexes with the influenza virus and are able to efficiently compete with natural cell membrane targets. However, significant multivalent effects were observed even with as few as 6 ligands in a multivalent array. It is important to note that sulfated hPG **4** had only a very minor inhibitory effect at concentrations above 1 mM emphasizing the importance of the SA unit as a specific ligand for HA.

Fusion Inhibition. Secondly, we investigated the ability of influenza A (strain A/X31) virus to undergo fusion using fluorescence de-quenching of R18 upon fusion of labeled viruses with erythrocyte ghost membranes. Hemagglutinin is the major surface protein of influenza and mediates binding to the cell surface. After endocytosis the low pH in late endosomal compartments leads to a conformational change of HA which subsequently triggers fusion of the viral envelope with the endosomal membrane.

For the experimentation, viruses were labeled as mentioned already above with R18 incorporated into the viral membrane at self quenched concentration. The monomeric form of sialic acid had a small effect on the fluorescence de-quenching and reduced the extent of fusion by 15% at our highest measured concentration of 4 mM. However, all tested sialic acid functionalized polymers had a more pronounced effect on virus fusion. hPGs **1**–**3** reduced the extent of fusion to 35% at 4 mM sugar equivalents; 50% inhibition was achieved at approximately 2 mM sugar equivalents. There were no significant differences observed in multivalency effects within the hPG series **1**–**3**, which differ only by degree of functionalization. As with the binding inhibition study, nPG **5** was the most effective, causing almost total inhibition at 4 mM SA equivalent concentration; 50% inhibition could be achieved below 100 μM sugar equivalents. On a per sugar basis, nanogel **5** was found to be approximately 20 fold more effective than the hPG series **1**–**3** at causing 50% inhibition. Again, sulfated polymer **4**[35] showed no effect. It must be highlighted that the fusion assay reflects the fusion of all bound viruses whose number was also strongly reduced (Figure 4). For instance, nPG **6** reduced the binding by 40% at 1 mM. Furthermore the same concentration reduced the fusion by 20%. This means that only ~50% of the viruses were able to bind and fuse for this particular case.

Fusion kinetics. In addition, we examined the kinetics of the fusion process by fitting the exponential phase between acidification and triton addition (Figure 5). This reflects the sum of de-quenching of all individual viruses. Fitting reveals the time constant, which gives information about the time at which 50% of bound viruses have been fused and by this about the efficiency of the HA induced fusion process. We found a time constant of 50 sec in case of the control, which was preincubated in the absence of any inhibitor. In contrast, as shown in Figure 4 the samples that were preincubated with multivalent inhibitors showed a strong deceleration of the fusion reaction. After 1 and 4 mM sugar equivalents hPG **3** the time constant increased to 100 sec and 310 sec, respectively. On per sugar basis, the same amount of nPG **5** led to an increase of the time constant to 630 and 700 sec, respectively. The multivalent inhibitors had a significant effect on the kinetics of the fusion being up to 14 times slower than the control. Hence, viral particles that were able to bind to the ghost's membrane still have contact to the inhibitor which prevents the normal time scale fusion we observed in the control samples.

Inhibition of infection. For a successful infection of a host cell the virus has to enter via endocytosis and deliver its genomic material after fusion with the endosomal membrane. To

investigate whether our designed polymers have an impact on viral infectivity we preincubated unlabeled virus with different amounts of polymers and exposed MDCK cells at a multiplicity of infection (MOI) of 25. The production of viral proteins is a clear sign for a successful infection. We assayed the production of viral nucleoprotein (NP) by immunofluorescence microscopy and flow cytometry using anti–NP antibodies. Using both techniques, six hours post-infection we detected NP protein signal in 80–90% of the cells which indicates a positive infection (Figure 6A). At this stage of infection we mostly got a strong nuclear and cytoplasmic signal which gave the best signal to noise ratio compared to background fluorescence of uninfected cells and allowed a clear discrimination of infected and uninfected cells. Using viruses treated with multivalent inhibitors we obtained a strong reduced NP signal (Figure 6B). 1 mM sugar equivalents of nPG **5** reduced the amount of infected cells to 20% of the control level. An increase of the concentration to 4 mM led only to a small increase of inhibition (< 15% of control level).

Conclusion

In summary, a new class of multivalent glycoarchitectures of a previously unreported size (50–70 nm) was introduced, which provide a powerful inhibitor of influenza virus activity. We compared two different length scales which differ in particle size and the multiplicity of sugar units. The inhibitory activities of the polymeric glycoconjugates drastically increase with nanoparticle size. Comparing the inhibition of binding and fusion nPG **5** (50 nm) is $7 \cdot 10^3$ times more effective than hPG **1** (3 nm) at comparable sugar concentrations. A further increase in functionalization of nPGs (**6** vs. **5**) did not lead to a better inhibition but to a reduced activity down to the level of hPG. Also, we present evidence that the optimal multivalent inhibitor **5** reduces the viral activity by up to 80%, which emphasizes the importance of matching sizes and multiplicity for biological surface interactions. We show that both size and ligand density play important roles in enhancing the inhibition of infection.

Experimental Section

Materials, viruses, cells. Influenza A (H3N2) virus (strain A/X31) was prepared on eggs as previously described.[39] For each experiment the virus was diluted to 1 mgml^{-1} and treated with different inhibitors. Madine-Darby Canine Kidney cells (MDCK) were cultured in DMEM (10% FCS, 1% P/S) with passage every 3-4 days. For infection experiments the cells were trypsinized one day prior to infection and seeded in 35 mm petri dishes. Human erythrocytes from healthy donors were purchased from the local Blood Bank (Charité, Berlin). Octadecylrhodamine B (R18) was purchased from Molecular Probes (Invitrogen, USA). Phosphate buffered saline was used for all dilutions during the experiments.

Binding assay. Influenza A (strain A/X31) virus was labeled with octadecylrhodamine B (R18) as follows. The virus was diluted to a concentration of 1 mgml^{-1} in PBS and incubated with 20 µM R18 for 30 min at RT. Unbound R18 was removed via centrifugation 5 min at 25.000 g. The pellet was resuspended in PBS. 40 µl red blood cell suspension (approx. 10^8 cells) were mixed with 10 µl virus suspension and incubated at RT for 20 min. Unbound virus was removed by 5 min, 5000 rpm centrifugation. The pellet was resuspended in PBS and the fluorescence per red blood cell was detected by flow cytometry using a Beckton Dickinson FACScan flow cytometer. The data was acquired using BD CellQuest.

Fusion assay. Fusion was measured by monitoring the fluorescence dequenching (FDQ) of the lipid like fluorophore R18 upon fusion of R18-labeled viruses with ghost membranes (18). For this 10 µl labeled virus suspension was mixed with 40 µl ghost suspensions and incubated 20 min at RT. Unbound virus was removed by 5 min, 5000 rpm centrifugation. The virus-ghost suspension was transferred to a glass cuvette containing pre-warmed sodium acetate buffer and the fluorescence was detected (λ_{ex}= 560 nm; λ_{em}= 590 nm) using a Horiba Yobin Yvon FluoroMax spectrofluorometer. Fusion was triggered by the addition of 15 µl citric acid (0.25 mM). The suspension was stirred continuously with a 2- by 8-mm Teflon coated magnetic stir bar. After 600 s the fusion was stopped by adding 50 µl Triton X-100 (final concentration 0.5%) to obtain maximum R18 fluorescence. The percentage of FDQ was calculated as described previously:[40]

$$FDQ = \frac{F(t) - F(0)}{F(max) - F(0)} \cdot 100\ \%$$

where F(0) and F(t) are the fluorescence intensity before starting fusion and the fluorescence intensity at a given time (t), respectively.

Infection. Influenza A virus (strain A/X31) was diluted in PBS containing 0.2% BSA and added to MDCK cells at MOI of 25. After 1h adhesion at 37°C unbound virus was removed and the cells were incubated in DMEM (0.2% BSA) for 6 h. For microscopy the cells were fixed in 2% formaldehyde, permeabilized in 0.5% Triton X-100 and immunolabeled using anti–NP first antibody (Mouse IgG2a, influenza A, 1 mgml^{-1}, Chemicon/MP) and antiMouse Cy2 secondary antibody (Goat IgG, λ_{ex}= 490 nm; λ_{em}= 508 nm, Amersham). Fluorescence microscopy was carried out using an Olympus FV1000 confocal microscope. For flow cytometry the cells were scrapped from the Petri dish and fixed in 2% formaldehyde. The cells were permeabilized with saponin and immunolabeled as described above. The fluorescence per cell was measured using a Beckton Dickinson FACScan flow cytometer.

Cryo–electron microscopy (Cryo–TEM)

Sample preparation. Droplets of the corresponding sample solution (nPG–OH with 130 mgml^{-1} in water and azido–nPG with 30 mgml^{-1} in water/methanol) were applied to perforated (1 µm hole diameter) carbon film covered 200 mesh grids (R1/4 batch of Quantifoil Micro Tools GmbH, Jena, Germany), which had been hydrophilized prior to use by 60 s plasma treatment at 8 W in a BALTEC MED 020 device. The supernatant fluid was removed with a filter paper until an ultrathin layer of the sample solution was obtained spanning the holes of the carbon film. The samples were immediately vitrified by propelling the grids into liquid ethane at its freezing point (90 K) operating a guillotine like plunging device.

Electron microscopy. The vitrified samples were transferred under liquid nitrogen into a Tecnai F20 FEG transmission electron microscope (FEI Company, Oregon, USA) using the Gatan (Gatan Inc., California, USA) cryoholder and stage (Model 626). Microscopy was carried out at 94 K sample temperature using the microscopes low dose protocol at a calibrated primary magnification of 62,000× and an accelerating voltage of 160 kV (FEG-illumination). Images were recorded using an EAGLE 2k-CCD device (FEI Company, Oregon, USA) at full 2048 by 2048 pixel size. Due to the very low contrast of the polymer particles an unusual high defocus value of 10 µ was necessary for imaging. (Figure 2)

Materials and Methods

All reagents and solvents were purchased from commercial suppliers and used without further purification. Reactions requiring dry or oxygen free conditions were carried out under argon using Schlenck glassware. ^{1}H and ^{13}C NMR spectra were recorded on ECX 400 (400 MHz and 100 MHz for ^{1}H and ^{13}C, respectively) spectrometer at 25^{o}C. Chemical shifts δ are given in parts per million (ppm) and the spectra

were calibrated using the deuterated solvent peak. The molecular weights, molecular weight distribution of the polymers were determined by size-exclusion chromatography (SEC) on PSS Agilent 1100 system with three Suprema (10 µm) columns (3×ID8.0×300 mm) using water (0.05% NaN_3) as eluent. The system was calibrated by narrow pullulan standards (M_w range: 1080–6.41×10^5 $gmol^{-1}$) using a PSS Win-GPC software. Dynamic light scattering (DLS) measurements of the various polymers were conducted using a NanoDLS particle sizer (Brookhaven Instruments Corp.) at 25°C. Aqueous samples were filtered through 0.2 µm filters prior to analysis. Water of Millipore quality was used in all experiments. Naturally occurring sialic acids constitute a family of more than 50 structurally distinct nine-carbon 3-deoxy-ulosonic acids, the most widespread derivative being 5-*N*-acetyl-neuraminic acid (Neu5Ac). We used the abbreviation of sialic acid (SA) for Neu5Ac. Hyperbranched polyglycerols were synthesized by following reported procedure.[27a, 41] The polymer was characterized by NMR, SEC, and MALDI for the determination of absolute molecular weights, and polydispersity (M_w/M_n). The nPGs were prepared after recently published procedure.[36c]

Compound 4 (hPG-OSO_3Na). It was prepared according to the procedure of Türk.[35] ^{1}H NMR (500 MHz, D_2O, δ): 4.72 (s, primary C$\underline{H}_2$OSO_3Na), 4.37, 3.84–3.52 (m, hPG backbone), 1.40 (m, C$\underline{H}_2$–hPG starter unit), 0.80 (t, C$\underline{H}_3$–hPG starter unit); ^{13}C{^{1}H} NMR (125 MHz, D_2O, δ): 78.3, 77.3, 75.9, 70.5, 69.4, 68.3, 67.2, 66.9; IR (KBr): ν(cm^{-1})= 3470 (ν-OH), 2922, 2871 (m, ν-CH_3, ν-CH_2), 1260 (S=O), 816 (C–O–S). Sulfur content was determined by elemental analysis (S: 20.4%). Degree of functionalization (DF) was 85%.

Synthesis of hPG- and nPG-Sialic Acid Conjugates. hPG-sialic acid conjugates were prepared by the click reaction of hPG-alkynes with complementary azido-C_{11}-SA. The conversion of hydroxyl groups on hPG into the alkyne functionality[34] was confirmed by the appearance of a medium and a weak alkyne C–H stretching band in the IR spectrum at 3288 and 2113 cm^{-1}, respectively, as well as by NMR analysis. All 3 functionalities (15%, 50%, and 90%) had similar NMR spectra except for the change in peak intensity; it was higher as DF increased. Representative ^{1}H and ^{13}C NMR spectra of the conjugates are shown in the supporting information.

Alternatively, nPG-SA possessing the reversed linkage functionality, that is the propargyl group installed on the sialic acid residue and the azido group on the nPG scaffold, was also similarly prepared to investigate the effect of size and functionalities on influenza virus binding and fusion. Advantageously, nanoparticles (50 nm in size) may be formed that still bear a significant quantity of residual epoxide groups by heating the reaction for reduced time.[36c] These epoxide groups can undergo a standard ring opening reaction with sodium azide to provide a facile route to 12% azide functionalized nPG. These nanogels with up to 0.12 azide units per glycerol repeat unit in the final product were used as substrates for further reactions with sialic acid. For the synthesis of 80% azide functionalized nPGs a two step modification procedure was used to convert the hydroxyl groups on nPG into mesyl groups, followed by nucleophilic substitution with sodium azide. Particle sizes were determined by dynamic light scattering (DLS) and transmission electron microscopy (TEM) (see Figure 2).

The SA clusters were obtained, as previously mentioned via copper catalyzed Sharpless/Huisgen click reaction. After completion of the reaction, determined by IR measurements, the mixture was extracted with ethyl acetate, washed with EDTA sat. solution, water and brine. After drying, solvent was removed in vacuo and the residue was purified by dialysis/ ultrafiltration in acetone. The acetylated products were deprotected by using NaOMe in MeOH, and finally saponificated with 0.1 M NaOH solution. After the reaction, the mixture was dialyzed against water for 4 days (MWCO 1 and 5 kDa) with frequent changes in water. In case of nPG derivatives ultrafiltration was used (MWCO 10 kDa). The final products were obtained by lyophilization and characterized by ^{1}H and ^{13}C NMR analysis. The sialic acid density was determined from ^{1}H NMR integration of different peaks and the absolute molecular weight of hPG derivatives was determined by SEC. All SA functionalized hPGs and nPGs had similar NMR spectra except for the change in peak intensity; it was higher as DF increased.

Compound 1–3 protected. ^{1}H NMR (500 MHz, $CDCl_3$, δ): 7.64 (m, C=C$\underline{H}$), 5.41–4.63 (m, SA, $\underline{H}$–8, $\underline{H}$–7, N$\underline{H}$, $\underline{H}$–4), 4.41–3.28 (m, $\underline{H}$–9, $\underline{H}$–5, $\underline{H}$–6, –OC$\underline{H}_3$, –C$\underline{H}_2$–, and hPG backbone), 2.58 (m, SA, $\underline{H}$–3e), 2.10–1.82 (m, SA, OAcs, $\underline{H}$–3a), 1.59–1.19 (m, –C$\underline{H}_2$–); ^{13}C{^{1}H} NMR (125 MHz, $CDCl_3$, δ): 175.1–171.2 (O=C SA, NHAc, OAcs), 169.3 (C–1, SA), 146.1 (C=CH), 125.8 (C=CH), 98.7 (C–2, SA); 78.2–63.9 (hPG backbone, SA, C–6, C–4, C–8), 52.4 (OC$\underline{H}_3$, SA), 51.6, 50.0 (C–5, SA), 38.2 (C–3), 29.8–20.1 (NHAc, OAcs, –C$\underline{H}_2$–, SA); IR (KBr): ν(cm^{-1}) = 3430 (br, ν-H_2O), 2921 (s, ν-CH_3, ν-CH_2), no peak at 3288 and 2114 (w, ν-C≡CH), 2104 (s, ν-N_3).

Compound 1–3 deprotected. ^{1}H NMR (500 MHz, D_2O, δ): 7.83 (m, C=C$\underline{H}$), 4.46–3.19 [(m, SA ($\underline{H}$–8, $\underline{H}$–7, $\underline{H}$–4, $\underline{H}$–9, $\underline{H}$–5, $\underline{H}$–6), –C$\underline{H}_2$–, and hPG backbone], 2.72 (m, SA, $\underline{H}$–3e), 1.89 (s, SA, NHAc), 1.50–1.17 (m, SA, $\underline{H}$–3a, –C$\underline{H}_2$–); ^{13}C{^{1}H} NMR (125 MHz, D_2O, δ): 175.1 (O=C, NHAc), 171.3 (C–1, SA), 146.1 (C=CH), 125.8 (C=CH), 99.1 (C–2, SA); 78.2–64.9 (hPG backbone, SA), 51.9, 51.2 (C–5, SA), 39.1 (C–3), 29.8–22.1 (NHAc, –C$\underline{H}_2$–, SA).

Compound 5, 6 protected. ^{1}H NMR (500 MHz, $CDCl_3$, δ): 7.56 (C=C$\underline{H}$), 5.40–5.25 (m, SA, $\underline{H}$–8, N$\underline{H}$, $\underline{H}$–7), 4.83 (m, SA, $\underline{H}$–4), 4.30–3.49 [m, SA ($\underline{H}$–9, $\underline{H}$–5, $\underline{H}$–6, OC$\underline{H}_3$ at 3.83) and nPG core], 3.43 (d, SC$\underline{H}_2$C=C), 2.68 (m, SA, $\underline{H}$–3e), 2.10–1.82 (m, NHAc, OAcs, $\underline{H}$–3a, SA); ^{13}C{^{1}H} NMR (125 MHz, $CDCl_3$, δ): 175.1–170.3 (C=O SA, NHAc, OAcs), 168.8 (SA, C–1), 144.5 (C=CH), 124.9 (C=CH), 84.9–84.0 (C–2, nPG backbone), 78.6 (SA, C–6), 74.9 (SA, C–4), 72.1 (SA, C–8), 68.8–68.2 (nPG, SA: C–7), 62.7 (SA, C–9), 52.5 (SA, OC$\underline{H}_3$), 51.7 (SA, C–5), 40.3 (SA, C–3), 23.3–21.8 (NHAc, OAcs); IR (KBr): ν(cm^{-1}) = 3441 (br, ν–OH), 2922 (s, ν–CH_3, ν–CH_2), no peaks at 3288 and 2114 (w, ν-C≡CH, SA) and 2102 (s, ν_{as}-N_3).

Compound 5, 6 deprotected. ^{1}H NMR (500 MHz, D_2O; δ) = 7.91 (C=C$\underline{H}$), 4.30–3.25 [m, SA ($\underline{H}$–8, N$\underline{H}$, $\underline{H}$–7, $\underline{H}$–4, $\underline{H}$–9, $\underline{H}$–5, $\underline{H}$–6); SC$\underline{H}_2$C=C; and nPG core], 2.79 (m, SA, $\underline{H}$–3e), 2.03 (s, SA, NHAc), 1.85 (SA, $\underline{H}$–3a).

Acknowledgments

This work was supported by the Fonds der Chemischen Industrie (doctoral fellowship to I.P.) and the Deutsche Forschungsgemeinschaft (SFB 765).

Keywords: influenza virus, multivalent inhibition, nanogels polyglycerol, sialic acid

[1] R. G. Webster, W. J. Bean, O. T. Gorman, T. M. Chambers, Y. Kawaoka, *Microbiol. Mol. Biol. Rev.* **1992**, *56*, 152-179.
[2] K. Subbarao, T. Joseph, *Nat. Rev. Immunol.* **2007**, *7*, 267-278.
[3] J. C. Dyason, M. von Itzstein, *Aust. J. Chem.* **2001**, *54*, 663-670.
[4] a) J. Beigel, M. Bray, *Antiviral Res.* **2008**, *78*, 91-102; b) I. Carlescu, D. Scutaru, M. Popa, C. Uglea, *Med. Chem. Res.* **2009**, *18*, 477-494; c) F. G. Hayden, *Antiviral Res.* **2006**, *71*, 372-378.
[5] M. Matrosovich, H.-D. Klenk, *Rev. Med. Virol.* **2003**, *13*, 85-97.
[6] W. Weis, J. H. Brown, S. Cusack, J. C. Paulson, J. J. Skehel, D. C. Wiley, *Nature* **1988**, *333*, 426-431.
[7] M. Mammen, S.-K. Choi, G. M. Whitesides, *Angew. Chem. Int. Ed.* **1998**, *37*, 2754-2794.
[8] T. J. Pritchett, J. C. Paulson, *J. Biol. Chem.* **1989**, *264*, 9850-9858.
[9] E. G. Weinhold, J. R. Knowles, *J. Am. Chem. Soc.* **1992**, *114*, 9270-9275.
[10] a) G. D. Glick, J. R. Knowles, *J. Am. Chem. Soc.* **1991**, *113*, 4701-4703; b) G. D. Glick, P. L. Toogood, D. C. Wiley, J. J. Skehel, J. R. Knowles, *J. Biol. Chem.* **1991**, *266*, 23660-23669; c) Z. Gan, R. Roy, *Tetrahedron* **2000**, *56*, 1423-1428; d) S. Sabesan, J. Duus, P. Domaille, S. Kelm, J. C. Paulson, *J. Am. Chem. Soc.* **1991**, *113*, 5865-5866; e) S. Sabesan, J. O. Duus, S. Neira, P. Domaille, S. Kelm, J. C. Paulson, K. Bock, *J. Am. Chem. Soc.*

1992, *114*, 8363-8375; f) T. Ohta, N. Miura, N. Fujitani, F. Nakajima, K. Niikura, R. Sadamoto, C.-T. Guo, T. Suzuki, Y. Suzuki, K. Monde, S.-I. Nishimura, *Angew. Chem. Int. Ed.* **2003**, *42*, 5186-5189.

[11] a) S. J. Meunier, R. Roy, *Tetrahedron Lett.* **1996**, *37*, 5469-5472; b) A. Marra, M.-C. Scherrmann, A. Dondoni, R. Ungaro, A. Casnati, P. Minari, *Angew. Chem. Int. Ed.* **1995**, *33*, 2479-2481; c) Z. Gan, R. Roy, *Can. J. Chem.* **2002**, *80*, 908-916; d) S. A. Kalovidouris, O. Blixt, A. Nelson, S. Vidal, W. B. Turnbull, J. C. Paulson, J. F. Stoddart, *J. Org. Chem.* **2003**, *68*, 8485-8493.

[12] a) A. Marra, L. Moni, D. Pazzi, A. Corallini, D. Bridi, A. Dondoni, *Org. Biomol. Chem.* **2008**, *6*, 1396-1409; b) K. Fujimoto, O. Hayashida, Y. Aoyama, C.-T. Guo, K. I. P. J. Hidari, Y. Suzuki, *Chem. Lett.* **1999**, *28*, 1259-1260.

[13] A. B. Tuzikov, A. A. Chinarev, A. S. Gambaryan, V. A. Oleinikov, D. V. Klinov, N. B. Matsko, V. A. Kadykov, M. A. Ermishov, I. y. V. Demin, V. V. Demin, P. D. Rye, N. V. Bovin, *ChemBioChem* **2003**, *4*, 147-154.

[14] a) R. Roy, C. A. Laferrière, *Can. J. Chem.* **1990**, *68*, 2045-2054; b) R. Roy, C. A. Laferrière, *J. Chem. Soc., Chem. Commun.* **1990**, 1709-1711; c) K. I. P. J. Hidari, T. Murata, K. Yoshida, Y. Takahashi, Y.-h. Minamijima, Y. Miwa, S. Adachi, M. Ogata, T. Usui, Y. Suzuki, T. Suzuki, *Glycobiology* **2008**, *18*, 779-788; d) M. Ogata, K. I. P. J. Hidari, W. Kozaki, T. Murata, J. Hiratake, E. Y. Park, T. Suzuki, T. Usui, *Biomacromolecules* **2009**, *10*, 1894-1903.

[15] Y. Makimura, S. Watanabe, T. Suzuki, Y. Suzuki, H. Ishida, M. Kiso, T. Katayama, H. Kumagai, K. Yamamoto, *Carbohydr. Res.* **2006**, *341*, 1803-1808.

[16] a) M. Llinares, R. Roy, *Chem. Commun.* **1997**, 2119-2120; b) K. Matsuoka, H. Oka, T. Koyama, Y. Esumi, D. Terunuma, *Tetrahedron Lett.* **2001**, *42*, 3327-3330; c) S. J. Meunier, Q. Wu, S.-N. Wang, R. Roy, *Can. J. Chem.* **1997**, *75*, 1472-1482; d) R. Roy, D. Zanini, S. J. Meunier, A. Romanowska, *J. Chem. Soc., Chem. Commun.* **1993**, 1869-1872; e) D. Zanini, R. Roy, *J. Org. Chem.* **1996**, *61*, 7348-7354; f) J. J. Landers, Z. Cao, I. Lee, L. T. Piehler, P. P. Myc, A. Myc, T. Hamouda, A. T. Galecki, J. R. B. Jr, *J. Infect. Dis.* **2002**, *186*, 1222-1230; g) J. D. Reuter, A. Myc, M. M. Hayes, Z. Gan, R. Roy, D. Qin, R. Yin, L. T. Piehler, R. Esfand, D. A. Tomalia, J. R. Baker, *Bioconjugate Chem.* **1999**, *10*, 271-278; h) D. Zanini, R. Roy, *J. Am. Chem. Soc.* **1997**, *119*, 2088-2095; i) J.-I. Sakamoto, T. Koyama, D. Miyamoto, S. Yingsakmongkon, K. I. P. J. Hidari, W. Jampangern, T. Suzuki, Y. Suzuki, Y. Esumi, T. Nakamura, K. Hatano, D. Terunuma, K. Matsuoka, *Bioorg. Med. Chem.* **2009**, *17*, 5451-5464.

[17] a) C.-T. Guo, X.-L. Sun, O. Kanie, K. F. Shortridge, T. Suzuki, D. Miyamoto, K. I.-P. J. Hidari, C.-H. Wong, Y. Suzuki, *Glycobiology* **2002**, *12*, 183-190; b) J. E. Kingery-Wood, K. W. Williams, G. B. Sigal, G. M. Whitesides, *J. Am. Chem. Soc.* **1992**, *114*, 7303-7305; c) A. Reichert, J. O. Nagy, W. Spevak, D. Charych, *J. Am. Chem. Soc.* **1995**, *117*, 829-830; d) W. Spevak, J. O. Nagy, D. H. Charych, M. E. Schaefer, J. H. Gilbert, M. D. Bednarski, *J. Am. Chem. Soc.* **1993**, *115*, 1146-1147.

[18] a) N. V. Bovin, A. B. Tuzikov, A. A. Chinarev, A. S. Gambaryan, *Glycoconj. J.* **2004**, *21*, 471-478; b) L. Bondioli, L. Costantino, A. Ballestrazzi, D. Lucchesi, D. Boraschi, F. Pellati, S. Benvenuti, G. Tosi, M. A. Vandelli, *Biomaterials* **2010**, *31*, 3395-3403; c) D. Lemoine, V. Préat, *J. Control. Rel.* **1998**, *54*, 15-27.

[19] R. Roy, F. O. Andersson, G. Harms, S. Kelm, R. Schauer, *Angew. Chem. Int. Ed.* **1992**, *31*, 1478-1481.

[20] a) S.-K. Choi, M. Mammen, G. M. Whitesides, *Chem. Biol.* **1996**, *3*, 97-104; b) W. J. Lees, A. Spaltenstein, J. E. Kingery-Wood, G. M. Whitesides, *J. Med. Chem.* **1994**, *37*, 3419-3433; c) M. Mammen, G. Dahmann, G. M. Whitesides, *J. Med. Chem.* **1995**, *38*, 4179-4190; d) G. B. Sigal, M. Mammen, G. Dahmann, G. M. Whitesides, *J. Am. Chem. Soc.* **1996**, *118*, 3789-3800; e) A. Spaltenstein, G. M. Whitesides, *J. Am. Chem. Soc.* **1991**, *113*, 686-687; f) M. A. Sparks, K. W. Williams, G. M. Whitesides, *J. Med. Chem.* **1993**, *36*, 778-783.

[21] a) N. Bovin, E. Korchagina, T. Zemlyanukhina, N. Byramova, O. Galanina, A. Zemlyakov, A. Ivanov, V. Zubov, L. Mochalova, *Glycoconj. J.* **1993**, *10*, 142-151; b) N. V. Bovin, *Glycoconj. J.* **1998**, *15*, 431-446; c) A. S. Gambaryan, E. Y. Boravleva, T. Y. Matrosovich, M. N. Matrosovich, H. D. Klenk, E. V. Moiseeva, A. B. Tuzikov, A. A. Chinarev, G. V. Pazynina, N. V. Bovin, *Antivir. Res.* **2005**, *68*, 116-123.

[22] M. N. Matrosovich, L. V. Mochalova, V. P. Marinina, N. E. Byramova, N. V. Bovin, *FEBS Lett.* **1990**, *272*, 209-212.

[23] W.-Y. Wu, B. Jin, G. Y. Krippner, K. G. Watson, *Bioorg. Med. Chem. Lett.* **2000**, *10*, 341-343.

[24] S.-K. Choi, M. Mammen, G. M. Whitesides, *J. Am. Chem. Soc.* **1997**, *119*, 4103-4111.

[25] A. Tsuchida, K. Kobayashi, N. Matsubara, T. Muramatsu, T. Suzuki, Y. Suzuki, *Glycoconj. J.* **1998**, *15*, 1047-1054.

[26] a) T. Furuike, S. Aiba, T. Suzuki, T. Takahashi, Y. Suzuki, K. Yamada, S.-I. Nishimura, *J. Chem. Soc., Perkin Trans. 1* **2000**, 3000-3005; b) K. Matsuoka, C. Takita, T. Koyama, D. Miyamoto, S. Yingsakmongkon, K. I. P. J. Hidari, W. Jampangern, T. Suzuki, Y. Suzuki, K. Hatano, D. Terunuma, *Bioorg. Med. Chem. Lett.* **2007**, *17*, 3826-3830; c) Z.-Q. Yang, E. B. Puffer, J. K. Pontrello, L. L. Kiessling, *Carbohydr. Res.* **2002**, *337*, 1605-1613; d) K. Suzuki, J.-I. Sakamoto, T. Koyama, S. Yingsakmongkon, Y. Suzuki, K. Hatano, D. Terunuma, K. Matsuoka, *Bioorg. Med. Chem. Lett.* **2009**, *19*, 5105-5108.

[27] a) A. Sunder, R. Hanselmann, H. Frey, R. Mulhaupt, *Macromolecules* **1999**, *32*, 4240-4246; b) R. Haag, A. Sunder, J. F. Stumbé, *J. Am. Chem. Soc.* **2000**, *122*, 2945-2955.

[28] a) B. I. Voit, A. Lederer, *Chem. Rev.* **2009**, *109*, 5924-5973; b) M. Calderón, M. A. Quadir, S. K. Sharma, R. Haag, *Adv. Mater.* **2010**, *22*, 190-218.

[29] G. R. Whittaker, *Exp. Rev. Mol. Med.* **2001**, *3*, 1-13.

[30] a) R. K. Kainthan, M. Gnanamani, M. Ganguli, T. Ghosh, D. E. Brooks, S. Maiti, J. N. Kizhakkedathu, *Biomaterials* **2006**, *27*, 5377-5390; b) R. K. Kainthan, S. R. Hester, E. Levin, D. V. Devine, D. E. Brooks, *Biomaterials* **2007**, *28*, 4581-4590; c) J. Khandare, A. Mohr, M. Calderón, P. Welker, K. Licha, R. Haag, *Biomaterials* **2010**, *31*, 4268-4277.

[31] C. Siegers, M. Biesalski, R. Haag, *Chem. Eur. J.* **2004**, *10*, 2831-2838.

[32] a) A. Dworak, W. Walach, B. Trzebicka, *Macromol. Chem. Phys.* **1995**, *196*, 1963-1970; b) R. Tokar, P. Kubisa, S. Penczek, A. Dworak, *Macromolecules* **1994**, *27*, 320-322.

[33] E. J. Vandenberg, *J. Polym. Sci., Part A: Polym. Chem.* **1985**, *23*, 915-949.

[34] I. Papp, J. Dernedde, S. Enders, R. Haag, *Chem. Commun.* **2008**, 5851-5853.

[35] H. Türk, R. Haag, S. Alban, *Bioconjugate Chem.* **2004**, *15*, 162-167.

[36] a) K. Landfester, *Angew. Chem. Int. Ed.* **2009**, *48*, 4488-4507; b) A. L. Sisson, R. Haag, *Soft Matter* **2010**, -; c) A. L. Sisson, D. Steinhilber, T. Rossow, P. Welker, K. Licha, R. Haag, *Angew. Chem. Int. Ed.* **2009**, *48*, 7540-7545.

[37] a) W. H. Binder, R. Sachsenhofer, *Macromol. Rapid Commun.* **2007**, *28*, 15-54; b) V. V. Rostovtsev, L. G. Green, V. V. Fokin, K. B. Sharpless, *Angew. Chem. Int. Ed.* **2002**, *41*, 2596-2599.

[38] G.-J. Boons, A. V. Demchenko, *Chem. Rev.* **2000**, *100*, 4539-4566.

[39] T. Korte, K. Ludwig, Q. Huang, P. Rachakonda, A. Herrmann, *Eur. Biophys. J.* **2007**, *36*, 327-335.

[40] R. Blumenthal, A. Bali-Puri, A. Walter, D. Covell, O. Eidelman, *J. Biol. Chem.* **1987**, *262*, 13614-13619.

[41] A. Sunder, R. Mülhaupt, R. Haag, H. Frey, *Adv. Mater.* **2000**, *12*, 235-239.

Received: ((will be filled in by the editorial staff))
Published online: ((will be filled in by the editorial staff))

Figure Caption

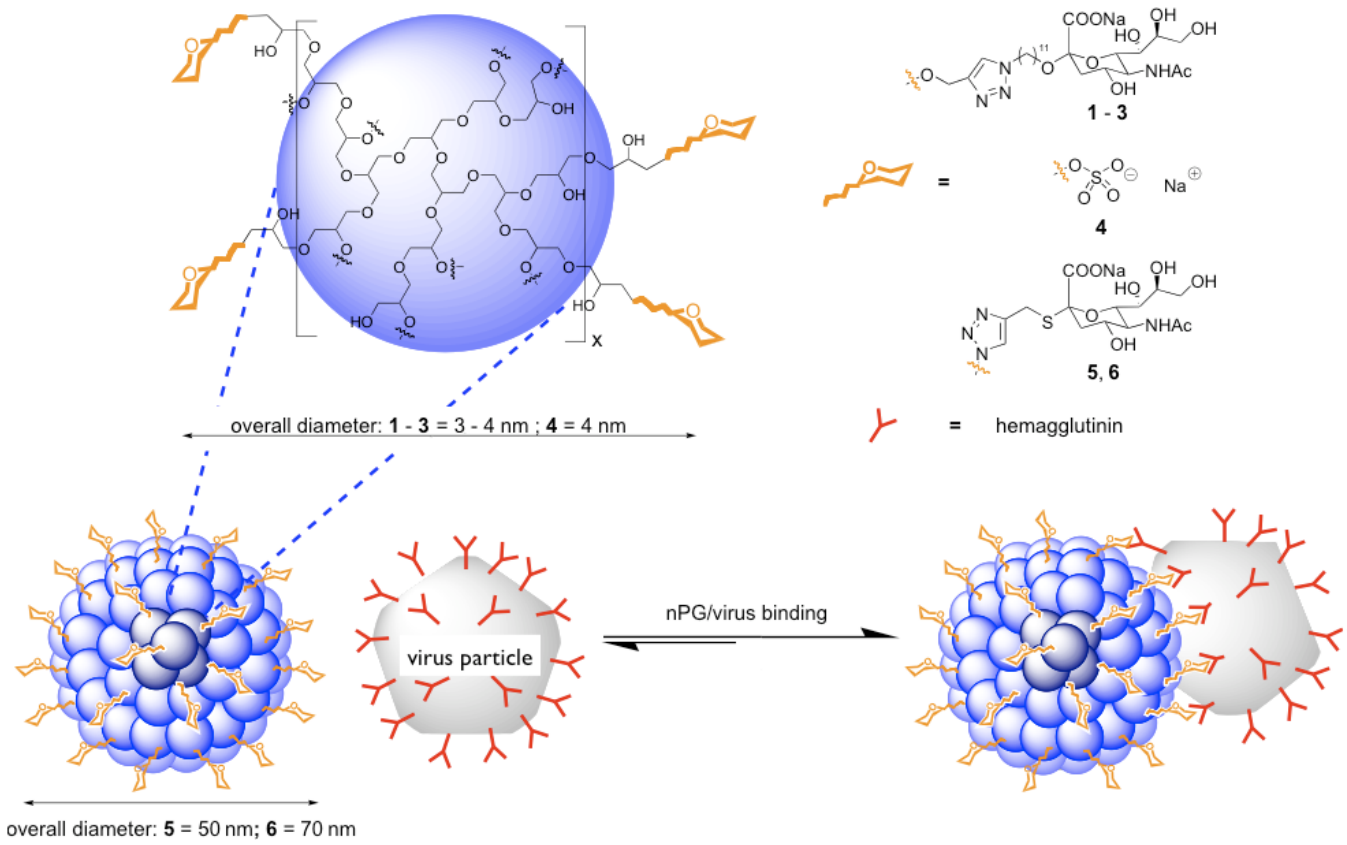

Figure 1. Schematic representation of functional polymeric nanoparticles. The PG structure is representative and only shows a small fragment of the actual nanoparticles.

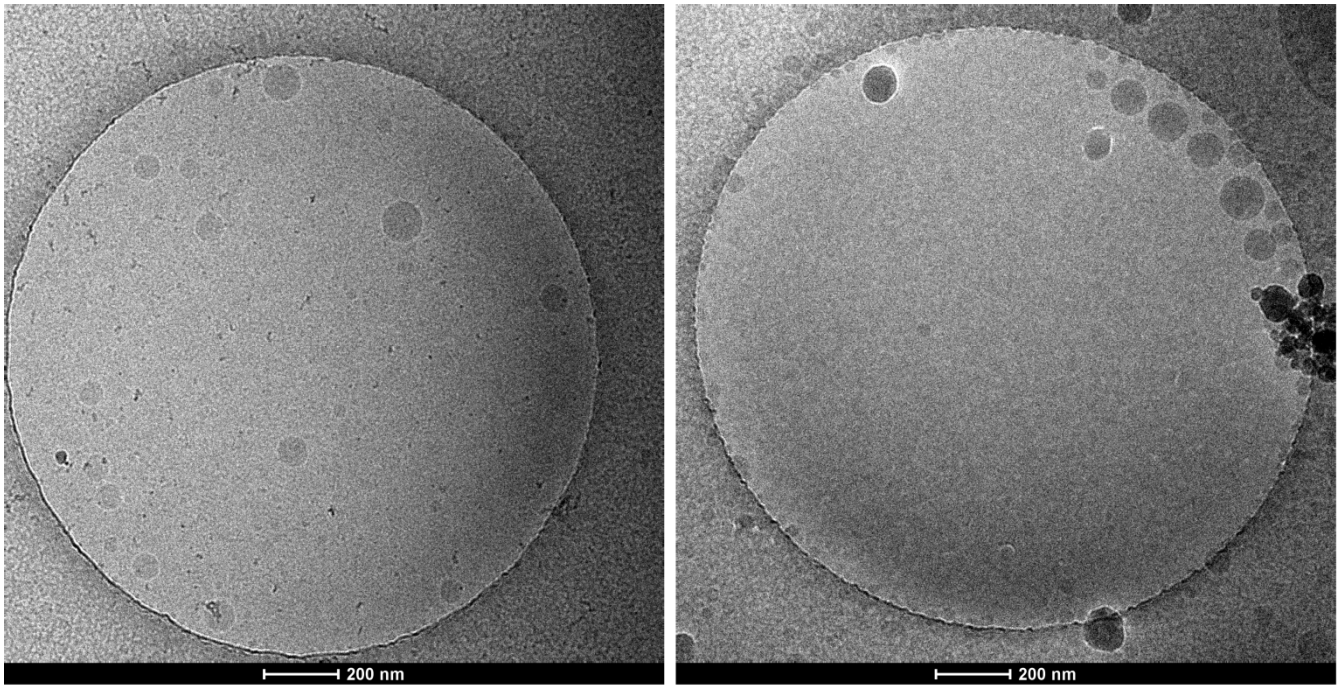

Figure 2. Cryo–TEM images of (left) nPG–OH (130 $mgml^{-1}$ in water) and (right) azido–nPG (30 $mgml^{-1}$ in water/methanol) showing spherical particles with an average diameter of 50 nm, respectively; scale bar 200 nm.

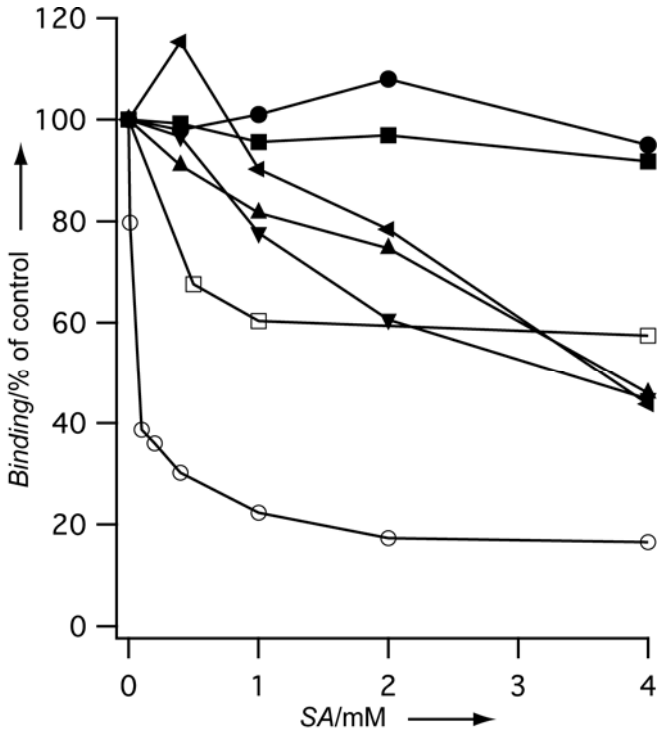

Figure 3. Relative binding efficiency of influenza A (strain A/X31) virus to human red blood cells dependent on the applied concentration of inhibitor. The virus was preincubated with the noted amounts of hPG **1** (◄), hPG **2** (▼), hPG **3** (▲), hPG **4** (■), sialic acid (●), nPG **5** (○), nPG **6** (□).

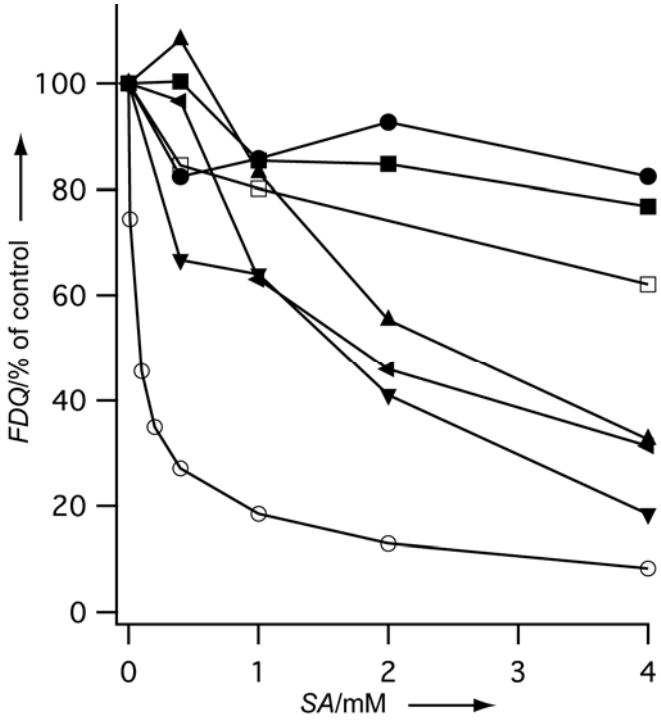

Figure 4. Fusion efficiency of influenza A (strain A/X31) virus with human red blood cell ghosts dependent on the applied concentration of inhibitor. The virus was preincubated with the noted amounts of hPG **1** (◄), hPG **2** (▼), hPG **3** (▲), hPG **4** (■), sialic acid (●), nPG **5** (○), nPG **6** (□).

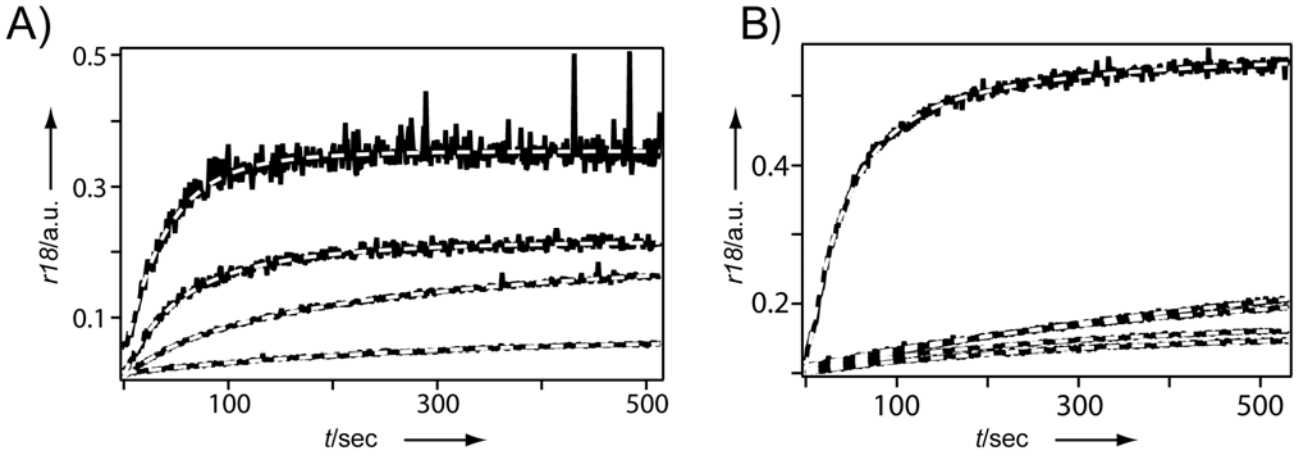

Figure 5. The kinetics of the fusion was recorded (black) and fitted with an exponential function (white dashed line). Shown are the curves of the control sample and virus preincubated with A) 1–4 mM hPG **2** and B) 0.4–4 mM nPG **5**.

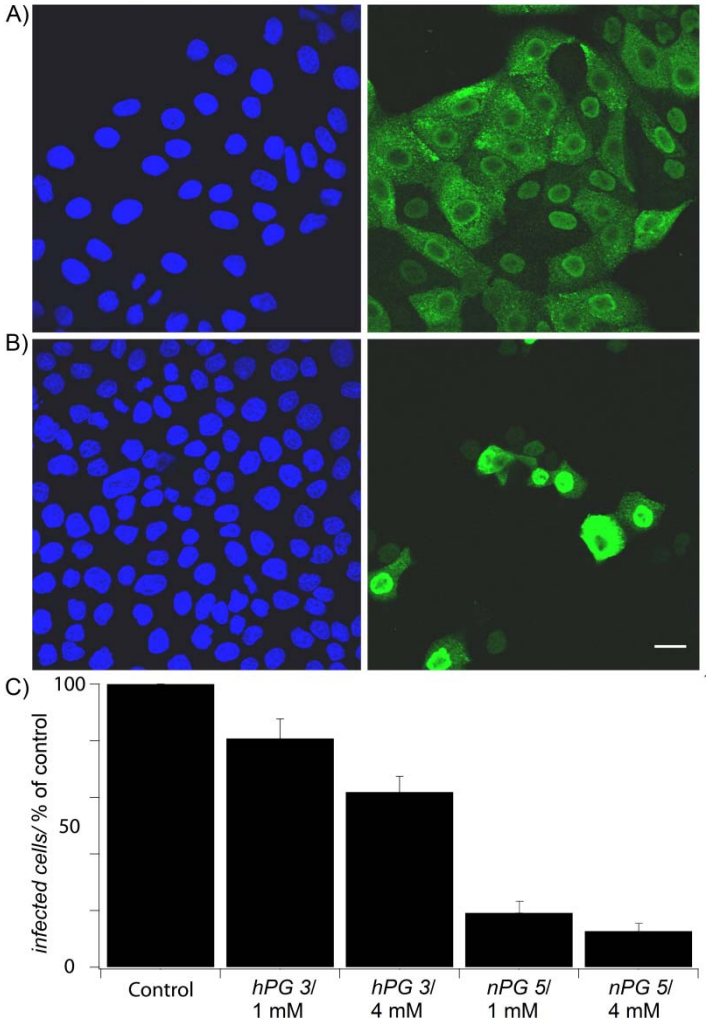

Figure 6. MDCK cells were infected with influenza A (strain A/X31) virus without A) and after preincubation with 4 mM nPG **5** B). The left two pictures show the nuclei stained with 4',6-diamidino-2-phenylindole (DAPI, blue). The viral nucleoprotein (NP) was detected with anti–NP antibody and visualized with a Cy2 linked secondary antibody. Only the cells that were successfully infected show a positive Cy2 signal. Scale bar: 10 µm; C) The amount of infected cells was quantified by flow cytometry.

Table 1. Characterization of hPG–SA and nPG–SA

PG derivatives	M_n [kDa][a]	Size [nm][b]	DF [%][c]	Sugar units/ polymer	IC_{50} [μM][e]	
					Binding	Fusion
1	6.6	3±0.1	15	6	365 [$2.19 \cdot 10^3$]	153 [$0.92 \cdot 10^3$]
2	14.4	3±0.7	50	20	69 [$1.38 \cdot 10^3$]	59 [$1.18 \cdot 10^3$]
3	23	3±1.3	90	35	62.9 [$2.2 \cdot 10^3$]	48 [$1.68 \cdot 10^3$]
4	6.5	4±1.1	85	0[d]	n.d.	n.d.
5	8,000	50±5.6	12	10,000	0.0058 [58]	0.008 [80]
6	27,000	70±6.8	80	60,000	0.0066 [400]	0.0143 [860]

[a] hPG: average molecular weight 3 kDa was used; M_w/M_n= 1.18; DB (degree of branching)= 0.57. Postfunctionalized M_n calculated using the M_n of the polyglycerol core and the experimental degree of functionalization. [b] Determined from DLS (water), the values represent the means of at least three experiments; ±standard deviation. [c] Determined by ^{1}H NMR analysis. [d] Dendritic polyglycerol sulfate as comparison (*cf.* Ref.[35]); n.d. not determined due to weak inhibition. [e] Values in parentheses represent IC_{50} values in micromolar concentrations based on a monomeric sugar unit concentration.

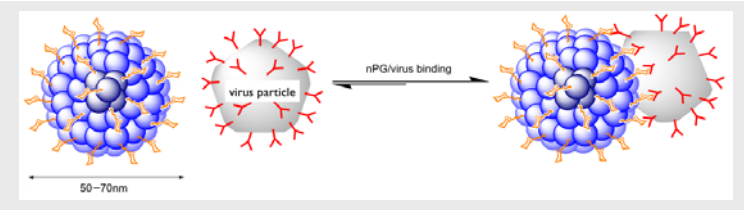

Polyglycerol nanoparticles were coated with sialic acid residues to afford excellent inhibitors of influenza virus binding, fusion and hence infectivity of erythrocytes. The evidence provided points clearly to a multivalent binding between nanoparticles and hemagglutinin rich virus surfaces; optimum nanoparticle size and surface ligand densities were identified. This approach highlights the versatility and potential of a growing class of biocompatible branched polyether nanogels, which benefit from a highly functionalizable, hydrophilic surface.

*I. Papp, C. Sieben, A. L. Sisson, J. Kostka, C. Böttcher, K. Ludwig, A. Herrmann, R. Haag**

Page No. – Page No.

Inhibition of Influenza Virus Activity by Multivalent Glycoarchitectures with Matched Sizes